

Improved image display by identifying the RGB family color space

Elvis Togban^a, Djemel Ziou^a,

^a *Département d'Informatique, Faculté des Sciences, 2500 Bl. de l'université, Université de Sherbrooke, J1K2R1, Sherbrooke, Québec, Canada.*

Abstract

To display an image, the color space in which the image is encoded is assumed to be known. Unfortunately, this assumption is rarely realistic. In this paper, we propose to identify the color space of a given color image using pixel embedding and the Gaussian process. Five color spaces are supported, namely Adobe RGB, Apple RGB, ColorMatch RGB, ProPhoto RGB and sRGB. The results obtained show that this problem deserves more efforts.

Keywords: Color reproduction, image display, Color space identification, RGB color space

1. Introduction

Colors are the subjective responses linked to psychological and physiological aspects of the human visual system when stimulated to radiation of the spectrum with frequencies that extend from 450 THz to 750 THz [1]. Based on the tristimulus color theory, color space is a color representation

Email addresses: E.Togban@usherbrooke.ca (Elvis Togban), Djemel.Ziou@usherbrooke.ca (Djemel Ziou)

system usually based on a set of triplets. RGB color spaces are the most used color space for images display on electronic devices and on the Web. The RGB family is composed of the channels Red, Green and Blue. In order to faithfully reproduce color in different human activities (displaying, photography, industry), several variants of RGB have emerged such as Adobe RGB, ProPhoto RGB and sRGB. Moreover, color space can affect computer-based application such as skin detection [2, 3], facial age estimation [4] and image segmentation [5], white balancing [6]. Choosing an appropriate color space for a specific visual task is not easy knowing that an infinite number of color spaces can exist. In some applications or image display systems, the color space in which an image is encoded is assumed to be known. This assumption is rarely realistic. For example, the color space used by default on the Web is sRGB while most professional-level digital cameras use Adobe RGB. However, after editing an image, it is possible to embed the color space in the metadata. Once this information is available, the display device faithfully reproduces the colors of the image. However, after various operations on the image, the metadata can be missing or corrupted which will lead to a misrepresentation of the image. Figure 1 shows two images displayed by using the browser Firefox. Browsers consider that the image to be displayed is encoded in the sRGB color space. However, from left to right, each image is encoded respectively in sRGB, Apple RGB, and ProPhoto RGB. The color space is assumed to be unknown in the first two rows, so there is missing data allowing to carry out the transformation from the space in which the image

is encoded to the sRGB space. In other words, regardless of the color space in which the image is encoded, Firefox considers it as encoded in sRGB. As a result, there is a noticeable difference between the three images. In the last row, the color space is known. Therefore, the right transformation is used to convert the images from the color space in which it is encoded to sRGB. As a result, the color reproduction is more faithful for the three color spaces in which the image to be displayed is encoded.



Figure 1: Images displayed with Firefox browser. In the first two rows, the color spaces used for encoding the images are unknown, while those of the images in the last row are known.

In this paper, we are interested in the identification of an image color space. This problem was first addressed by Vezina et al. [7]. In their work, they used gamut estimation to discriminate between sRGB, HSV, HLS and Lab color spaces. Unfortunately, in the case of the RGB family, we need a more accurate estimation of the gamut. In this work, we use a feature based on pixels embedding and gaussian process. Five RGB color space namely Adobe RGB, Apple RGB, ColorMatch RGB, ProPhoto RGB and sRGB are considered. The paper is structured as follows. In the next section, we present our method for color space identification. Section 3 is devoted to the model estimation. The experimental results are described in section 4.

2. Color space identification model

RGB color space family can be characterized by the gamut, the white point, the three primaries (Red, Green, and Blue) and the transfer function. All these attributes could be used to discriminate color spaces of the RGB family. The gamut and the white point can be estimated from images [7]. Unfortunately, at the best of knowledge, there is no available algorithm for the estimation of primaries and transfer function from images. Additionally, for the RGB family, the gamut estimators lack sufficient precision to reliably identify an image's color space. Instead, we propose pixel embedding and Gaussian process for color space identification. Let I be a color image encoded in a color space $C_1C_2C_3$ of the RGB family. Basically, the embedding consists in expressing a pixel value as a linear function of its adjacent pix-

els (in the same channel or in different channel). More precisely, the pixel embedding can be written as follows:

$$I_{k_1}(m, n) = \sum_{(i,j) \in V(m,n)} \gamma_{i,j,k_1} I_{k_2}(m+i, n+j) + r_{k_1,k_2}(m, n) \quad (1)$$

where γ_{i,j,k_1} are a set of coefficients such as $\gamma_{0,0,k_1} = 0$ if $k_1 = k_2$, $(k_1, k_2) \in \{C_1, C_2, C_3\} \times \{C_1, C_2, C_3\}$ refer to the channels of $C_1 C_2 C_3$, $I_{k_1}(m, n)$ is the value of the pixel located at (m, n) for the channel k_1 and $V(m, n)$ its neighborhood. A random variable $r_{k_1,k_2}(m, n)$ which is considered normally distributed with zero mean and standard deviation σ_{k_1,k_2} is associated with each location (n, m) and each pair (k_1, k_2) . We propose two possible embeddings namely the intra-channel embedding ($k_1 = k_2$) and the inter-channel embedding ($k_1 \neq k_2$). The parameters of the embedding model described in Eq. 1 are the standard deviation σ_{k_1,k_2} and the vector $\gamma_{k_1} = (\gamma_{i,j,k_1} \mid (i, j) \in V(m, n))^t$. The vector is formed by sweeping the neighborhood line by line starting from the top left. In this paper, the neighborhood is defined as $V(m, n) = \{(i, j) \mid -J \leq i, j \leq J\}$ where $(2J + 1)^2$ is the number of neighboring pixels of the pixel (m, n) .

Consider a collection of labeled images, where the label of an image is the color space in which it is encoded. For each image in this collection, we calculate an embedding vector for each channel in the case of intra-channel embedding and an embedding vector for each pair of channels in the case of inter-channel embedding by using the algorithm 1 described in the next sec-

tion. The three intra-channel (resp. six inter-channel) embedding vectors are concatenated to form an intra-channel (resp. inter-channel) feature vector. Note that, according to Eq. 1, the embedding vector γ_{k_1} does not depend on the spatial location (m, n) of the pixel. To summarize, the dimension of inter-channel and intra-channel feature vectors are respectively $6(2J+1)^2$ and $3((2J+1)^2 - 1)$ per image. The feature vectors are used to train multinomial logistic regression (MLR) as a classifier. The choice of MLR is motivated by the fact that it is frugal (less data is needed for training) and its result is easy to explain [8]. The number of classes is equal to the number of color spaces we need to identify. For the test, given a color image, the feature vector is estimated as explained before and the color space is identified by using the learned classifier.

3. Parameters estimation

For the sake of notational simplicity, in the following, σ_{k_1, k_2} and $r_{k_1, k_2}()$ will be denoted respectively σ and $r()$. For both inter-channel and intra-channel cases, Eq. 1 is equivalent to a linear regression model where $\{I_{k_2}(m+i, n+j)\}_{(i,j) \in V(m,n)}$ are the explanatory variables and $I_{k_1}(m, n)$ is the response variable. However, a given pixel may not be linearly correlated to its neighbors. In this case, the random variable $r(m, n)$ is not drawn from a Gaussian with zero mean. For the Red channel of a RGB image (fig. 2a), we illustrate the histogram of $r(m, n)$ (fig. 2b). As we can notice, the errors distribution look like a zero-mean Gaussian. To evaluate the scope of the

embedding described in Eq. 1, we estimated the histogram of the variable $r(n, m)$ using a channel or a pair of channels from an image and we performed a K-S Test to decide the normality of this variable $r(n, m)$. This procedure was performed using 1000 pictures of size 602×400 . We noticed that for all the images, the distribution of this error is not a Gaussian. In fact, the error distribution of $r(n, m)$ has a heavier tail and a higher peak than a Gaussian distribution. However, for a sub-sample of pixels, the error distribution of $r(n, m)$ can be a zero-mean Gaussian (fig. 2c). For our experiment with 1000 pictures, on average, the error is Gaussian for 36% pixels in the case of inter-channel and for 30 % pixels in the intra-channel case. The equation 1 is therefore valid for a subset of pixels.

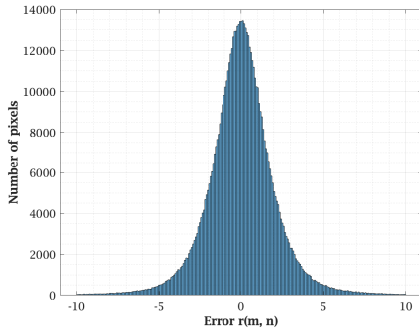
Let I_k ; $k \in \{C_1, C_2, C_3\}$ be a channel of I and the pixel $I_k(m, n)$ located at (m, n) can be embedded; that means $r_{k_1, k_2}(m, n)$ is a Gaussian variable. Let consider the complete data $\{(I_{k_1}(m, n), s(m, n, k_1, k_2))\}_{(m, n) \in V(m, n)}$, where $s(m, n, k_1, k_2) = s_0(m, n, k_1, k_2)$, $s_1(m, n, k_1, k_2)$ is the set of binary variables. By definition, $s_0(n, m, k_1, k_2) = 1$ (resp. $s_1(n, m, k_1, k_2) = 1$) indicates that the pixel $I_{k_1}(m, n)$ of the channel k_1 can (resp. cannot) be embedded over its neighbor of the channel k_2 . The complete likelihood is given by:

$$\mathcal{L} = \prod_{m, n} \prod_{b=0}^1 (\pi_b p(I_{k_1}(n, m) | s_b(n, m, k_1, k_2) = 1, \theta_{k_1 b}))^{s_b(n, m, k_1, k_2)} \quad (2)$$

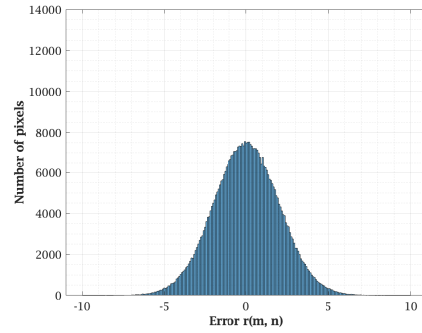
where $p(s_b(n, m, k_1, k_2) = 1) = \pi_b$ is the distribution over $s_b(n, m, k_1, k_2) = 1$.



(a)



(b)



(c)

Figure 2: (a) A RGB image. (b) Histogram of the errors $r(m, n)$ computed for the red channel of the image displayed in (a).

Let us recall that when $s_0(m, n, k_1, k_2) = 1$, $r_{k_1, k_2}(m, n)$ is a normal random variable, which leads to consider that $I_{k_1}(m, n)$ is drawn from a Gaussian with mean $a_1(m, n, k_1, k_2) = \sum_{(i, j) \in V(m, n)} \gamma_{i, j, k_1} I_{k_2}(m + i, n + j)$ and variance σ^2 :

$$p(I_{k_1}(m, n) \mid s_0(m, n, k_1, k_2) = 1, \theta_{k_1 0}) = \mathcal{N}(I_{k_1}(m, n) \mid a_1(m, n, k_1, k_2), \sigma^2) \quad (3)$$

where the parameter vector $\theta_{k_1 0} = (\gamma_{k_1}, \sigma)^t$ are those of the vector γ_{k_1} , σ . If $s_1(m, n, k_1, k_2) = 1$, the channel $I_{k_1}(m, n)$ is supposed to be drawn from a

Gaussian mixture of M components:

$$p(I_{k_1}(m, n) \mid s_1(m, n, k_1, k_2) = 1, \theta_{k_1}) = \sum_{c=1}^M \alpha_c \mathcal{N}(I_{k_1}(m, n) \mid \mu_c, \lambda_c^2) \quad (4)$$

where the parameter vector $\theta_{k_1} = (\alpha_1, \mu_1, \lambda_1, \dots, \alpha_M, \mu_M, \lambda_M)^t$, $\sum_{c=1}^M \alpha_c = 1$, and $\alpha_c \geq 0$. We will now estimate the parameters θ_{k_1} by using the EM algorithm. Because the variables $s_b(m, n, k_1, k_2)$ are non-observable, instead of maximizing the logarithm of the complete-data likelihood in Eq. 2, we maximize its conditional expectation given by:

$$l = \sum_{m,n} \sum_{b=0}^1 \tau_b(m, n, k_1, k_2, \theta_{k_1 b}) \ln[\pi_b p(I_{k_1}(n, m) \mid s_b(m, n, k_1, k_2) = 1, \theta_{k_1 b})] \quad (5)$$

where $\tau_b(m, n, k_1, k_2, \theta_{k_1 b})$ is the conditional expectation of $s_b(m, n, k_1, k_2)$. The EM algorithm proceeds iteratively in two steps, expectation (E) and maximization (M). The E-step at the iteration η , consists in computing the posterior $\tau_b(m, n, k_1, k_2, \theta_{k_1 b})$.

$$\begin{aligned} \tau_b(m, n, k_1, k_2, \theta_{k_1 b}^{(\eta)}) &= p(s_b(m, n, k_1, k_2) = 1, \theta_{k_1 b}^{(\eta)} \mid I_{k_1}(m, n)) \\ &= \frac{\pi_b^{(\eta)} p(I_{k_1}(m, n) \mid s_b(m, n, k_1, k_2) = 1, \theta_{k_1 b}^{(\eta)})}{\sum_{b=0}^1 \pi_b^{(\eta)} p(I_{k_1}(m, n) \mid s_b(m, n, k_1, k_2) = 1, \theta_{k_1 b}^{(\eta)})} \end{aligned} \quad (6)$$

The M-Step requires maximizing Eq. 5 with respect to $\theta_{k_1 b}$. By setting the partial derivative with respect to these variables to zero and solving we

obtain:

$$\pi_b^{(\eta+1)} = \sum_{m,n} \frac{\tau_b(m, n, k_1, k_2, \theta_{k_1 b}^{(\eta)})}{N} \quad (7)$$

where N is the number of pixels.

$$\sigma^{2(\eta+1)} = \frac{\sum_{m,n} \tau_0(m, n, k_1, k_2, \theta_{k_1 b}^{(\eta)}) [I_{k_1}(m, n) - \sum_{(i,j)} \gamma_{i,j,k_1}^{(\eta)} I_{k_2}(m+i, n+j)]^2}{\sum_{m,n} \tau_0(m, n, k_1, k_2, \theta_{k_1 b}^{(\eta)})} \quad (8)$$

For the parameter vector γ_{k_1} , we have to solve the following equation:

$$A^{(\eta)} \gamma_{k_1}^{(\eta+1)} = Y^{(\eta)} \quad (9)$$

where A is a symmetric matrix with

$$A^{(\eta+1)} = \begin{pmatrix} a_{-J,-J,-J,-J} & a_{-J,-J,-J,-J+1} & \cdots & a_{-J,-J,J,J} \\ a_{-J,-J,-J,-J+1} & a_{-J,-J+1,-J,-J+1} & \cdots & a_{J,J,-J,-J+1} \\ \vdots & \vdots & \ddots & \vdots \\ a_{-J,-J,-J,J} & a_{-J,-J+1,-J,J} & \cdots & a_{J,J,-J,J} \\ a_{-J,-J,-J+1,-J} & a_{-J,-J+1,-J+1,-J} & \cdots & a_{J,J,-J+1,-J} \\ \vdots & \vdots & \ddots & \vdots \\ a_{-J,-J,J,J} & a_{-J,-J+1,J,J} & \cdots & a_{J,J,J,J} \end{pmatrix} \quad (10)$$

where

$$a_{i,j,u,v}^{(\eta)} = \sum_{m,n} \tau_0(m, n, k_1, k_2, \theta_{k_1 b}^{(\eta)}) I_{k_2}(m+i, n+j) I_{k_2}(m+u, n+v) \quad (11)$$

$$\begin{aligned}
\gamma_k^{(\eta+1)} &= \begin{pmatrix} \gamma_{-J,-J,k_1}^{(\eta+1)} \\ \gamma_{-J,-J+1,k_1}^{(\eta+1)} \\ \vdots \\ \gamma_{-J,J,k_1}^{(\eta+1)} \\ \gamma_{-J+1,-J,k_1}^{(\eta+1)} \\ \vdots \\ \gamma_{J,J,k_1}^{(\eta+1)} \end{pmatrix} \\
Y^{(\eta)} &= \begin{pmatrix} \sum_{m,n} \tau_0(m,n,k_1,k_2,\theta_{k_1b}^{(\eta)}) I_{k_1}(m,n) I_{k_2}(m-J,n-J) \\ \sum_{m,n} \tau_0(m,n,k_1,k_2,\theta_{k_1b}^{(\eta)}) I_{k_1}(m,n) I_{k_2}(m-J,n-J+1) \\ \vdots \\ \sum_{m,n} \tau_0(m,n,k_1,k_2,\theta_{k_1b}^{(\eta)}) I_{k_1}(m,n) I_{k_2}(m-J,n+J) \\ \sum_{m,n} \tau_0(m,n,k_1,k_2,\theta_{k_1b}^{(\eta)}) I_{k_1}(m,n) I_{k_2}(m-J+1,n-J) \\ \vdots \\ \sum_{m,n} \tau_0(m,n,k_1,k_2,\theta_{k_1b}^{(\eta)}) I_{k_1}(m,n) I_{k_2}(m+J,n+J) \end{pmatrix} \quad (12)
\end{aligned}$$

Again we use the EM for the estimation of the parameters θ_{k_1} of the Gaussian mixture (second level of the EM). Consider the complete data $\{(I_k(m,n), z(m,n))^t\}_{(m,n) \in V(m,n)}$, where a single component of the vector $z(m,n)$ of dimension M is one; i.e. $z(m,n) = (0, \dots, 1, \dots, 0)^t$. A vector $z(m,n)$ indicates the component from which $I_k(m,n)$ originates; $p(I_k(m,n) | z_c(m,n) = 1, \theta_{k_1}) = \mathcal{N}(I_{k_1}(m,n) | \mu_c, \lambda_c^2)$ and $p(z_c(m,n) = 1) = \alpha_c$. The conditional

expectation of the logarithm of the complete-data likelihood is given by:

$$l_2 = \sum_{m,n} \tau_1(m, n, k_1, k_2, \theta_{k_1 b}) \sum_{c=1}^M \iota_c(m, n, k_1, \theta_{k_1 1}) \ln[\alpha_c p(I_{k_1}(n, m) | z_c(m, n) = 1, \theta_{k_1 1})] \quad (13)$$

where $\iota_c(m, n, k_1, \theta_{k_1 1})$ is the conditional expectation of $z_c(m, n, k_1)$. Note that, if one center of the Gaussian mixture coincides with a sample observation and the corresponding variance tends to zero, then the likelihood function increases without limit, leading to a degenerate EM estimator. For this, we consider that all the components of the Gaussian mixture have the same variance; $\lambda_c^2 = \lambda^2$. In the E-step, we estimate the conditional posterior:

$$\begin{aligned} \iota_c(m, n, k_1, \theta_{k_1 1}^{(\eta)}) &= p(z_c(m, n) = 1, \theta_{k_1 1}^{(\eta)} | I_{k_1}(m, n)) \\ &= \frac{\alpha_c^{(\eta)} p(I_{k_1}(m, n) | z_c(m, n) = 1, \theta_{k_1 1}^{(\eta)})}{\sum_{c=1}^C \alpha_c^{(\eta)} p(I_{k_1}(m, n) | z_c(m, n) = 1, \theta_{k_1 1}^{(\eta)})} \end{aligned} \quad (14)$$

In the M step, the following updating rules of the mixture parameters are obtained by maximizing the conditional expectation of the complete-data log-likelihood in Eq. 13:

$$\alpha_c^{(\eta+1)} = \frac{\sum_{m,n} \tau_1(m, n, k_1, k_2, \theta_{k_1 b}^{(\eta)}) \iota_c(m, n, k_1, \theta_{k_1 1}^{(\eta)})}{\sum_{m,n} \tau_1(m, n, k_1, k_2, \theta_{k_1 b}^{(\eta)})} \quad (15)$$

$$\lambda^{2(\eta+1)} = \frac{\sum_{m,n} \tau_1(m, n, k_1, k_2, \theta_{k_1 b}^{(\eta)}) \sum_{c=1}^M \iota_c(m, n, k_1, \theta_{k_1 1}^{(\eta)}) (I_{k_1}(m, n) - \mu_c^{(\eta)})^2}{\sum_{m,n} \tau_1(m, n, k_1, k_2, \theta_{k_1 b}^{(\eta)})} \quad (16)$$

$$\mu_c^{(\eta+1)} = \frac{\sum_{m,n} \tau_1(m, n, k_1, k_2, \theta_{k_1b}^{(\eta)}) \iota_c(m, n, k_1, \theta_{k_11}^{(\eta)}) I_{k_1}(m, n)}{\sum_{m,n} \tau_1(m, n, k_1, k_2, \theta_{k_1b}^{(\eta)}) \iota_c(m, n, k_1, \theta_{k_11}^{(\eta)})} \quad (17)$$

The parameters estimation procedure is summarized in algorithm 1.

Algorithm 1 Algorithm for the embedding

Input: I_{k_1} , I_{k_2} , and J .

Output: Return the embedding vector γ_{k_1} .

1. Initialization:

Randomly choose initial values of the parameters $\theta_{k_{10}}$ and use kmeans to initialize $\theta_{k_{11}}$.

2. E-step: For each pixel value $I_k(m, n)$, compute $\tau(m, n)$ (Eq. 6) and $\iota(m, n)$ (Eq. 14).

3. M-step: Estimate the parameters $\theta_{k_{10}}$ and $\theta_{k_{11}}$ by using Eqs. 7, 8, 9, 15, 16, 17.

4. Repeat the steps 2 and 3 until convergence.

4. Experimental Results

We collect 1000 images in RAW format respectively from each of DRES-DEN [9] and RAISE [10] collections. Then, we convert each image in five color spaces namely Adobe RGB, Apple RGB, ColorMatch RGB, ProPhoto RGB and sRGB. The number of images obtained is then 10K. Firstly, the embedding vectors are estimated from all images. The neighborhood is chosen by setting $J \in \{1, 2, 3\}$. In order to select the appropriate number of components M (Eq. 4), we use the Akaike information criterion (AIC). We vary M from 2 to 8 with step 2. Once the features have been extracted from each image, we use the Generalized discriminant analysis to reduce the

dimensions of the features [11]. We use them to train a multinomial logistic regression model (MLR). In our earlier work [12], we initially assumed that $I_{k_1}(m, n)$ was drawn from a uniform distribution. However, we have found that this distribution is not suitable. Therefore we compare our new approach to the one proposed in [12]. We also compare our model with the gamut estimation method [7]. For this purpose, we use 5k pixels per channel and per image (a total of 40 millions pixels) in order to approximate the gamut. In fact, in their work, the authors estimated the gamut by computing the histogram from a collection of images. We report the accuracy (in percentage) based on a five stratified cross-validation in table 1. The results reported are the obtained with $J = 2$ since it gives the highest accuracy. The following formula is used to compute the accuracy:

$$Accuracy(\%) = \frac{TD \times 100}{N} \quad (18)$$

where TD is the number of images with color space correctly detected and N is the total number of images in the test set.

As stated in section 2, the gamut estimation has to be more precise in order to discriminate between color space in the RGB family. Therefore, this method performs poorly (20.61%, see table 1). Our method outperforms by 2% ($\approx 68\%$) the one proposed in [12]. Indeed, the choice of Gaussian mixture to model the pixels that cannot be embedded over their neighbors is more suitable than a simple uniform distribution. It is worth noticing that the

Table 1: Accuracy obtained for the color space identification problem.

	Color Space	Accuracy by space (%)	Accuracy (%)
intra-channel	Adobe	69	68.59 \pm 1.34
	Apple	69.15	
	ColorMatch	66.6	
	ProPhoto	68.05	
	sRGB	70.15	
inter-channel RGB	Adobe	67.90	68.20 \pm 1.75
	Apple	68.30	
	ColorMatch	66.7	
	ProPhoto	67	
	sRGB	71.1	
intra-channel [12]	Adobe	67.55	66.31 \pm 1.28
	Apple	63.7	
	ColorMatch	66.05	
	ProPhoto	69.7	
	sRGB	64.55	
Gamut Estimation [7]	Adobe	20.65	20.61 \pm 1.18
	Apple	21.6	
	ColorMatch	22.7	
	ProPhoto	19.25	
	sRGB	18.85	

estimation of the embedding vector γ_{k_1} depend on the model of the pixels that cannot be embedded over their neighbors (see Eq. 5 - Eq. 12). According to the results, for both intra-channel and inter-channel embedding, the sRGB color space is the easiest to identify and the ColorMatch color space is the most difficult. The concatenation of the intra and inter channel embedding vectors, do not improve the identification.

5. Conclusion

This paper has proposed a model to identify RGB family color space. In order to identify the color space, we rely on pixel embedding and Gaussian process. When the metadata of an image does not have the information about the color space used, our model can be used to identify it. Once the color space is identified, we can produce a better display. When using our model, we were able to correctly identify the color space with an accuracy of 68%. Improvements can be made by choosing a more flexible distribution than the Gaussian one. In future work, we can also investigate if including image quality measure [13] can improve the color space detection.

References

- [1] A. Distante, C. Distante, *Color*, Springer International Publishing, Cham, 2020, pp. 79–176.
- [2] J. D. R. Khanam, P. Johri, Human skin color detection technique using different color models, *Trends and Advancements of Image Processing and Its Applications* (2022) 261–279.
- [3] I. Filali, D. Ziou, N. Benblidia, Multinomial bayesian kernel logistic discriminant based method for skin detection, in: *2012 Eighth International Conference on Signal Image Technology and Internet Based Systems*, IEEE, 2012, pp. 420–425.

- [4] J. Y. J. Hsieh, W. P. Boyce, E. Goddard, C. W. G. Clifford, Colour information biases facial age estimation and reduces inter-observer variability, *Research Square* (2022).
- [5] J. C. Canales, J. C. Canales, F. García-Lamont, A. Yee-Rendon, J. S. R. Castilla, L. R. Mazahua, Optimal segmentation of image datasets by genetic algorithms using color spaces, *Expert Systems with Applications* 238 (2024).
- [6] F. Kerouh, D. Ziou, K. Lahmar, Content-based computational chromatic adaptation, *Pattern Analysis and Applications* 21 (2018) 1109–1120.
- [7] M. Vezina, D. Ziou, F. Kerouh, Color space identification for image display, in: M. Kamel, A. Campilho (Eds.), *Image Analysis and Recognition*, Springer International Publishing, 2015, pp. 465–472.
- [8] R. Ksantini, D. Ziou, B. Colin, F. Dubeau, Weighted pseudometric discriminatory power improvement using a bayesian logistic regression model based on a variational method, *IEEE transactions on pattern analysis and machine intelligence* 30 (2) (2007) 253–266.
- [9] T. Gloe, R. Böhme, The 'dresden image database' for benchmarking digital image forensics, in: *Proceedings of the 2010 ACM Symposium on Applied Computing*, 2010, pp. 1584–1590.
- [10] D. T. Dang-Nguyen, C. Pasquini, V. Conotter, G. Boato, Raise: A raw

- images dataset for digital image forensics, in: Proceedings of the 6th ACM Multimedia Systems Conference, ACM, 2015, pp. 219–224.
- [11] G. Baudat, F. Anouar, Generalized discriminant analysis using a kernel approach, *Neural computation* 12 (10) (2000) 2385–2404.
- [12] E. Togban, F. Kerouh, D. Ziou, Identifying color space for improved image display, in: 2023 Twelfth International Conference on Image Processing Theory, Tools and Applications (IPTA), 2023, pp. 1–6.
- [13] L. Tang, L. Yuan, G. Zheng, Z. Wang, G. Zhai, Dtsn: No-reference image quality assessment via deformable transformer and semantic network, in: 2024 IEEE International Conference on Image Processing (ICIP), IEEE, 2024, pp. 1207–1211.